OPEN ACCESS
phytobiomesjournal.org
Phytobiomes Journal
A Transdisciplinary Journal of Sustainable Plant Productivity

RESEARCH

A *Streptomyces* Consortium Contributes Distinct Microbial Interactions During *Arabidopsis thaliana* Microbiome Assembly

Alexandra D. Gates,[1,2] Austin M. French,[1] Alexander A. Demetros,[2,3] Brittni R. Kelley,[2] and Sarah L. Lebeis[2,3,4,†]

[1] Department of Microbiology, University of Tennessee, Knoxville, TN
[2] Plant Resilience Institute, Michigan State University, East Lansing, MI
[3] Department of Microbiology and Molecular Genetics, Michigan State University, East Lansing, MI
[4] Department of Plant, Soil and Microbial Sciences, Michigan State University, East Lansing, MI

Accepted for publication 14 May 2023.

ABSTRACT

Although plant microbiome assembly involves a series of both plant–microbe and microbe–microbe interactions, the latter is less often directly tested. Here, we investigate a role for *Streptomyces* strains to influence assembly of other bacteria into root microbiomes through the use of two synthetic communities (SynComs): a 21-member community including four *Streptomyces* strains and a 17-member community lacking those *Streptomyces* strains. Following inoculation with these SynComs on wild-type *Arabidopsis thaliana* Col-0, differential abundance modeling on root endosphere 16S ribosomal RNA gene amplicon sequencing data revealed altered abundance of four diverse SynCom members: *Arthrobacter* sp. 131, *Agrobacterium* sp. 33, *Burkholderia* sp. CL11, and *Ralstonia* sp. CL21. Modeling results were tested by seedling coinoculation experiments with the four *Streptomyces* strains and differentially abundant members, which confirmed the predicted decreased abundance for *Arthrobacter* sp. 131, *Agrobacterium* sp. 33, and *Ralstonia* sp. CL21 when *Streptomyces* strains were present. We further characterized how the phytohormone salicylic acid (SA) mediates *Streptomyces* strains' influence over *Agrobacterium* sp. 33 and *Burkholderia* sp. CL11 seedling colonization. Although decreased colonization of *Ralstonia* sp. CL21 and *Arthrobacter* sp. 131 when *Streptomyces* spp. are present were not influenced by SA, direct antibiosis of *Arthrobacter* sp. 131 by *Streptomyces* was observed. These results highlight a role for *Streptomyces*-mediated microbial interactions during plant root microbiome assembly as well as distinct mechanisms that mediate them. Understanding the role of microbial interactions during microbiome assembly will inform the production of beneficial microbial treatments for use in agricultural fields.

Keywords: microbial interactions, plant microbiome assembly, salicylic acid, *Streptomyces*

[†]Corresponding author: S. L. Lebeis; lebeissa@msu.edu

Author contributions: A.D.G. and S.L.L. designed the SynCom experiment, coinoculation experiments, growth curves, and microbe–microbe assays. A.A.D. performed all experiments with help from co-authors. A.M.F. contributed to DNA extractions and seed production assays. A.D.G. contributed to coinoculation experiments and microbe–microbe assays. B.R.K. contributed to coinoculation experiments. Figures were generated by A.D.G. and S.L.L. A.D.G. and S.L.L. wrote the manuscript. A.D.G., A.A.D., B.R.K., and S.L.L. revised the manuscript.

Any opinions, findings, and conclusions or recommendations expressed in this material are those of the author(s) and do not necessarily reflect the views of the National Science Foundation.

Funding: This work is supported by two Directorate for Biological Sciences grants (DEB-1638922 and IOS-175017) to S. L. Lebeis.

e-Xtra: Supplementary material is available online.

The author(s) declare no conflict of interest.

Although plant root systems grow and develop within microbially rich soil, only a subset of microbes become members of the root microbiota. Roots form two major distinct root microbiomes: the external rhizosphere and the internal endosphere communities. Rhizosphere microbes live along the soil–root interface and respond to the root's physiology, while endosphere microbes colonize within the root tissue. These microbial communities confer benefits to the plant host through nutrient acquisition, pathogen protection, immune system priming, and stress tolerance (Trivedi et al. 2020). Assembly of these root microbiomes is shaped by both abiotic and biotic factors. Abiotic forces affecting assembly include soil composition and nutrient availability, while hosts and microbes each contribute biotic factors (Compant et al. 2019; Hassani et al. 2018). Of growing interest, microbial interactions in the soil or surrounding root systems also affect root microbiome composition (Boza et al. 2019). Although these factors are often elucidated separately, we predict that they act synergistically during microbiome assembly. Therefore, studies examining the intersection of microbe–microbe

and plant–microbe interactions are needed before the potential benefits of plant microbiomes can be realized.

The complexity of natural plant microbiomes poses a significant challenge to untangling plant–microbe from microbe–microbe interactions during microbiome assembly. Synthetic communities (SynComs) composed of characterized microbial strains provide a strategy to probe community assembly dynamics (Vorholt et al. 2017). Because the initial community composition of a SynCom inoculum is consistent between experimental replicates, this method represents a controlled and reproducible way to examine root microbiomes. Previous research utilizing SynComs with and without strains of interest has revealed important members of the microbiome, referred to as "keystone species", which affect total community composition (Carlström et al. 2019; Niu et al. 2017). Here, we use SynComs to concurrently examine microbe–microbe and plant–microbe interactions during root microbiome assembly and identify microbes that contribute to assembly processes.

Microbes influence plant root microbiome assembly by altering host plant physiology or directly affecting other potential microbiome members. Direct microbe–microbe interactions taking place in the soil and rhizosphere can be cooperative or competitive in nature (Hassani et al. 2018; Trivedi et al. 2020). Mechanisms of cooperation during microbiome assembly can involve nutrient exchange and molecular signaling (Hassani et al. 2018). Recently, a collection of rhizosphere-associated microbes was found to increase the colonization of a beneficial *Bacillus subtilis* strain in *Arabidopsis* roots (Eckshtain-Levi et al. 2020). Conversely, competition can occur via direct mechanisms such as antimicrobial production or indirect mechanisms such as niche competition (Hassani et al. 2018). Furthermore, systemic acquired resistance (SAR) and induced systemic resistance (ISR) are processes in which microbial colonization of plant leaves by pathogens for SAR or of roots by beneficial microbes for ISR initiate immune system responses to decrease subsequent pathogen colonization (Vlot et al. 2021). These mechanisms provide examples of indirect microbial interactions during microbiome assembly. However, the mechanisms by which microbial interactions among commensal organisms shape microbiome formation remain unclear (Hassani et al. 2018).

Numerous plant factors influence the assembly of root microbiomes, including species, genotype, tissue type, developmental stage, plant health, and immune system responses (Compant et al. 2019; Trivedi et al. 2020). Each of these factors uniquely alter leaf and root exudates to shape the environment that ultimately affects the microbial populations living in and around the plant (Trivedi et al. 2020). In aboveground and belowground *Arabidopsis thaliana* tissues, reactive oxygen species and production of phytohormones and phenolic compounds involved in the plant innate immune system are known to shape microbiomes (Bodenhausen et al. 2014; Lebeis et al. 2015; Pfeilmeier et al. 2021; Stringlis et al. 2018; Voges et al. 2019). For root endosphere microbiomes, the phytohormone salicylic acid (SA) modulates assembly (Lebeis et al. 2015). SA plays important roles in plant development as well as local and systemic responses to pathogens (Koo et al. 2020). Although SA coordinates plant responses, it also possesses antimicrobial activity (Adamczak et al. 2020). Furthermore, chemical crosstalk of the immune system can indirectly alter SA production and accumulation in plant tissues (Shigenaga et al. 2017). Currently, the weight of contribution of direct and indirect mechanisms of SA has not been elucidated for microbiome assembly.

Across plant species, the bacterial phyla *Proteobacteria*, *Bacteroidetes*, *Firmicutes*, and *Actinobacteria* dominate root microbiomes (Hacquard et al. 2015; Trivedi et al. 2020). Among *Actinobacteria*, the genus *Streptomyces* is a consistent member of the root endosphere in a variety of plants (Bulgarelli et al. 2012; Fitzpatrick et al. 2018; Lundberg et al. 2012). *Streptomyces* spp. have been identified in disease-suppressive soils and are known to prime the plant immune system (Cordovez et al. 2015; Vatsa-Portugal et al. 2017). *Arabidopsis* Col-0 seedling colonization by *Streptomyces* strains is directly influenced by SA, although there is no evidence that they use it as a carbon source during root colonization (Chewning et al. 2019; Worsley et al. 2021). Furthermore, *Streptomyces* spp. have vast biosynthetic capabilities, with the ability to affect other microbes via secondary metabolite production (Cordovez et al. 2015). These characteristics of *Streptomyces* make it a good candidate genus to examine the influence of microbial interactions during root community assembly. In this research, we utilized two SynComs (a 21-member community with four *Streptomyces* strains and a 17-member community lacking the *Streptomyces*) to examine the effect of these strains on community assembly in *Arabidopsis* genotypes. Although the SynComs were constructed to reflect dominate root microbiome members, plants inoculated with a slurry derived from natural soil (soil slurry) were included to confirm that root communities and plant outcomes are comparable among SynCom- and soil slurry-inoculated samples. Furthermore, our implemented experimental design allowed us to simultaneously explore the influence of the genus *Streptomyces* and plant production of SA during root endosphere microbiome assembly.

MATERIALS AND METHODS

Seed surface sterilization and germination. The *Arabidopsis* Col-0 and *sid2-2* (*sid2*) genotypes used in experiments outlined below were obtained from the *Arabidopsis* Biological Resource Center (https://abrc.osu.edu/). The genotype Col-0 is a wild-type *Arabidopsis* accession, while the *sid2* genotype is an isogenic mutant in Col-0 that does not accumulate SA due to a mutation in the isochorismate synthase gene (Wildermuth et al. 2001). Seeds were surface sterilized by treatment with 70% ethanol with 0.01% Triton X-100 for 1 min followed by treatment with freshly diluted 10% bleach for 12 min. Seeds were then washed four times with sterile deionized (DI) water. Seeds were stratified at 4°C in the dark for 3 days before plating on half-strength Murashige and Skoog (½MS) solid media with 1% sucrose and 8 g of Phytoagar. For SynCom Magenta jar experiments, seeds were germinated for 7 days in a reach-in growth chamber set to 22°C for 10 h of light and 18°C for 14 h of darkness. For monoinoculation and coinoculation plate experiments, seeds were germinated for 7 days at 22°C for 16 h of daylight and 18°C for 8 h of darkness for monoinoculation and coinoculation. The variation in growth conditions reflects longer light conditions to increase plant biomass for plate experiments. After seedlings were transferred into Magenta jars for SynCom experiments or plates for monoinoculation and coinoculation, the germination growth conditions were maintained for each experimental setup as stated above.

Soil slurry preparation. Field soil was collected from Mason Farm in Chapel Hill, NC, U.S.A. (35°53′30″N, 79°01′7″W). To generate the soil slurry inoculum, approximately 20 ml of soil was added to 100 ml of sterile DI water. The mixture was stirred uninterrupted for 1.5 h at room temperature on a magnetic stir plate. The soil slurry was removed from the magnetic stir plate and allowed to settle for 1 to 2 min. The resulting supernatant liquid above the sediment (20 ml) was collected and added to sterile freezer stock tubes with 20 ml of 60% glycerol, snap frozen in liquid nitrogen, and stored at −80°C. The day of inoculation, a freezer stock of soil slurry was thawed and centrifuged at 13,000 × *g* for 3 min. Glycerol-containing freezer stock medium was removed and

the soil slurry pellet were resuspended in sterile 1× phosphate-buffered saline (PBS). The optical density at 600 nm (OD_{600}) was measured using a spectrophotometer and soil slurry inoculum was normalized to an OD_{600} of 0.01 in 2-(*N*-morpholino)ethanesulfonic acid (MES)-buffered ½MS without sucrose. These resuspensions were used as "soil slurry" inoculum as described below.

SynCom selection and preparation. All bacterial isolates were grown in Lysogeny broth (LB) at 30°C in a shaking incubator at 150 rpm for 2 to 7 days, until cultures were turbid or displayed bacterial aggregates (Supplementary Table S1). Cultures were vortexed for 15 s to evenly suspend bacterial cells. Because our aim was to make the final OD_{600} of both communities 2, each member was diluted to OD_{600} of 0.095 for the 21-member community (SynCom I) and 0.118 for the 17-member community (SynCom II) in PBS. Community members were then mixed thoroughly and OD_{600} of the final SynComs was measured: 1.736 for SynCom I and 1.8 for SynCom II. Deviation from the desired final OD_{600} of 2 was due to variation in OD of cell cultures. SynCom aliquots were made with 2.5 ml of the community and 2.5 ml of glycerol in a 15-ml tube, snap frozen in liquid nitrogen, and stored at −80°C. For seedling inoculation, each SynCom aliquot was diluted in 1 liter of ½MS with 5 ml of MES buffer to obtain a final OD_{600} of 0.01. Seedlings were inoculated with 1 ml of the resulting SynCom I or SynCom II dilutions.

SynCom magenta jar experiments. For each replicate, one sterile Col-0 seedling was planted in a magenta jar containing 60 g of sterile calcine clay (Pro's Choice Rapid Dry) with 34 ml of half-strength MES-buffered MS with no sucrose, 15 ml of sterile DI water, and 1 ml of SynCom I, II, or soil slurry. Twenty-five replicates of each treatment were planted (SynCom I, SynCom II, or soil slurry). No-plant controls were unplanted jars inoculated the same way but did not contain any seedlings. Ten no-plant controls of each inocula type were set up. Five sterile control plants were planted in 60 g of sterile calcine clay with 35 ml of MES-buffered MS and 15 ml of sterile DI water and left uninoculated. Magenta jars were covered in gas-permeable BreathEasy film to exclude other microbes and maintain moisture throughout the experiment. Plants were grown in conditions stated above and no additional watering was necessary before plants were harvested after 2 or 4 weeks of growth.

During plant harvest, shoot and root tissue was separated using flame-sterilized scissors. Shoot tissue was weighed for biomass, snap frozen, and stored at −80°C. Root tissue was washed with 1 ml of phosphate buffer with 0.02% Silwet to remove calcine clay (Lebeis et al. 2015). To obtain endosphere samples, roots were then moved to a sterile 1.7-ml tube and washed three times in sterile DI water with 15 s of vortexing between each wash. Roots were moved to a new 1.7-ml tube and briefly centrifuged to remove excess water. Roots were weighed for biomass, snap frozen, and stored at −80°C. No-plant controls were harvested by suspending 2 ml of inoculated calcine clay in 2 ml of phosphate buffer with 0.02% Silwet (Lebeis et al. 2015) and vortexed for 10 s. Buffer was removed from clay, pelleted, snap frozen, and stored at −80°C. DNA extraction of root tissue was performed using the DNeasy Powersoil Kit (Qiagen) according to the manufacturer's instructions, with the modification of performing initial tissue homogenization in a SPEX SamplePrep Geno/Grinder 2010 for 20 min at 1,500 rpm. DNA was stored at −20°C until sequencing. To prepare SynCom and soil slurry inocula for DNA extraction, 5 or 15 ml of inocula, respectively, was pelleted in sterile 1.7-ml tubes. DNA extraction was performed on pellets of inocula and no-plant control samples by moving PowerBead Tube solution, garnet beads, and C1 solutions (Qiagen) to the 1.7-ml tubes containing sample pellets. Samples were then homogenized in a SPEX SamplePrep Geno/Grinder 2010 for 10 min at 1,500 rpm and the remaining DNA extraction protocol was performed according to the manufacturer's instructions.

In addition to root and shoot biomass measurements at the time of harvest for each inoculum type, seed production was assessed as a proxy for fitness that may occur due to the different inocula. Five replicates of sterile plant controls, soil slurry-inoculated plants, and SynCom-inoculated plants were uncovered and left to grow until siliques were produced. Once plants displayed developed green siliques, five siliques per plant were removed and seeds from all siliques were counted. This experiment was performed twice.

Amplicon library preparation and sequencing. The University of Tennessee Knoxville Genomics Core performed 16S ribosomal RNA (rRNA) gene amplicon library preparation using the Illumina preparation kit on DNA extracted from SynCom experiment samples. Primary PCRs were performed using primers 341F and 785R with a mixture of two peptide nucleic acids to amplify the V3 to V4 hypervariable regions but block plant mitochondrial and plastid sequences (Klindworth et al. 2013; Lundberg et al. 2013). Secondary PCRs were performed using Nextera XT forward and reverse primers to index each sample. Samples were sequenced on an Illumina MiSeq machine using version 3 chemistry and a 600-cycle flow cell for obtaining paired-end reads at 300 bp.

Amplicon sequence variant generation in DADA2. Sequencing reads were processed using DADA2 in RStudio. Briefly, quality profiles were examined, primer sequences were removed, and reads were trimmed to 260 bp for forward sequences and 230 bp for reverse sequences. After error rates were calculated, forward and reverse reads were merged. Amplicon sequence variants were inferred, and chimera sequences were removed. An amplicon sequence variant (ASV) count table for all samples was constructed for resulting sequences. Taxonomy was assigned using SILVA v138 for soil slurry samples and SynCom samples to identify potential contaminant reads from experimental setup, harvesting, or sequencing. Following assignment of non-SynCom member reads, SynCom samples were assigned taxonomy using a custom database of 16S rRNA gene sequences from SynCom members. For SynCom samples, ASVs corresponding to one SynCom member were combined. For figures, non-SynCom member ASVs were combined into the "other" column due to these ASVs being low in abundance. For soil slurry samples, all ASVs, including non-SynCom member ASVs, were maintained. Furthermore, for all samples, ASVs were filtered to those that had more than three read counts in at least three samples. Across all sample types, only samples with a total read count of 250 were used for analysis because the total read count for uninoculated control plants was not higher than 250. Although 20 replicates of all plant samples and 10 replicates of no-plant samples were sequenced, samples with less than 250 total reads were not included in our analysis, resulting in lower replicate number for some sample types, which are indicated in the corresponding figure legends. Relative abundance was calculated for soil slurry and SynCom samples by normalizing the ASV count to total read count for each individual sample.

Indicator species and CNVRG analysis of SynCom abundances. To identify poor and consistent colonizers among SynCom members, an indicator species analysis was applied to SynCom inocula, root samples, and no-plant controls using R package indicspecies with 50,000 permutations. Strains were categorized as "poor" colonizers if they were indicators of the SynCom I and SynCom II inocula but no other samples. Strains were categorized as "consistent" colonizers if they were indicators of root samples inoculated with both SynCom I and SynCom II. Dirichlet-multinomial modeling was performed on raw read counts for SynCom-inoculated samples only using the R package CNVRG, which was designed to be more sensitive to small changes in count data that

often occur in microbiome studies (Harrison et al. 2020). Read counts of zero were changed to 1 as instructed by the package. CNVRG normalized the SynCom member count data by sample sequencing depth, and sample estimates for p and pi values were extracted from the model and used for downstream analysis. Differential abundance testing built into the CNVRG package was then used to identify specific SynCom members with varying abundances between SynCom I- and SynCom II-inoculated root samples. Because we wanted to experimentally test model results, we again combined all non-SynCom member ASVs into a single "other" category to identify differentially abundant strains for downstream experiments.

Diversity calculations. Shannon's diversity index was calculated for all sample types using relative abundance calculations of ASVs with read counts above our selected threshold (including non-SynCom member ASVs) as described above for Figure 1 and Supplementary Figure S3. The diversity function (R package vegan) was used in RStudio with the index set to Shannon. A phylogenetic tree generated in Clustal Omega multiple sequence alignment (https://www.ebi.ac.uk/Tools/msa/clustalo/) using thresholded ASVs as described above (including non-SynCom member ASVs). Principal coordinate analysis was performed using the weighted Unifrac distance matrix generated in RStudio (R package phyloseq) from thresholded ASV abundances and the phylogenetic tree.

Phylogenetic tree construction. A phylogenetic tree for SynCom members was made using the Joint Genome Institute Integrated Microbial Genomes and Microbiomes (JGI IMG) (https://img.jgi.doe.gov) for Figure 2 and Supplementary Figure S4. The tree was constructed by adding gene *rpoB* from each SynCom isolate to the gene cart. Multiple sequence alignment was performed using Clustal Omega tool in JGI IMG. The Newick file for tree was downloaded and edited using Interactive Tree of Life (https://itol.embl.de).

Coinoculation experiments. Based on results from differential abundance testing, four SynCom members were found to have differential abundance between SynCom I and SynCom II root samples: *Arthrobacter* sp. 131, *Agrobacterium* sp. 33, *Burkholderia* sp. CL11, and *Ralstonia* sp. CL21. The four differential strains and the four *Streptomyces* strains were individually grown in liquid LB media in a 30°C shaking incubator set to 150 rpm for 2 to 7 days, until cultures were turbid or displayed bacterial aggregates. Monoinoculations of *Arthrobacter* sp. 131, *Agrobacterium* sp. 33, *Burkholderia* sp. CL11, and *Ralstonia* sp. CL21 were performed by diluting each member to an OD_{600} of 0.01 in sterile 1× PBS. Inoculations of only the four *Streptomyces* mixtures were performed by diluting each strain to an OD_{600} of 0.025 in sterile 1× PBS. Coinoculations of *Arthrobacter* sp. 131, *Agrobacterium* sp. 33, *Burkholderia* sp. CL11, and *Ralstonia* sp. CL21 with the four *Streptomyces* mixtures were performed by diluting each strain to an OD_{600} of 0.020 and mixing one of the first four SynCom members with the four *Streptomyces* to reach a final OD_{600} of 0.1. Each inoculum (150 µl) was spread on 120-by-120-mm square petri plates containing quarter-strength MS solid media with no sucrose. Five 7-day-old *Arabidopsis* seedlings of genotypes Col-0 or *sid2-2* were aseptically placed on each plate. Sterile control plates contained only five sterile seedlings. Plates were wrapped in Parafilm and arranged vertically in a growth chamber. Plates were left to grow for 2 or 4 weeks before harvest.

To harvest tissue, all five plants were removed from the plate with sterile tweezers and placed in a sterile 5-ml tube. Plants were weighed to obtain biomass and washed three times with sterile DI water, with 15 s of vortexing between each wash. Plants were then homogenized in 1 ml of sterile 1× PBS with approxi-

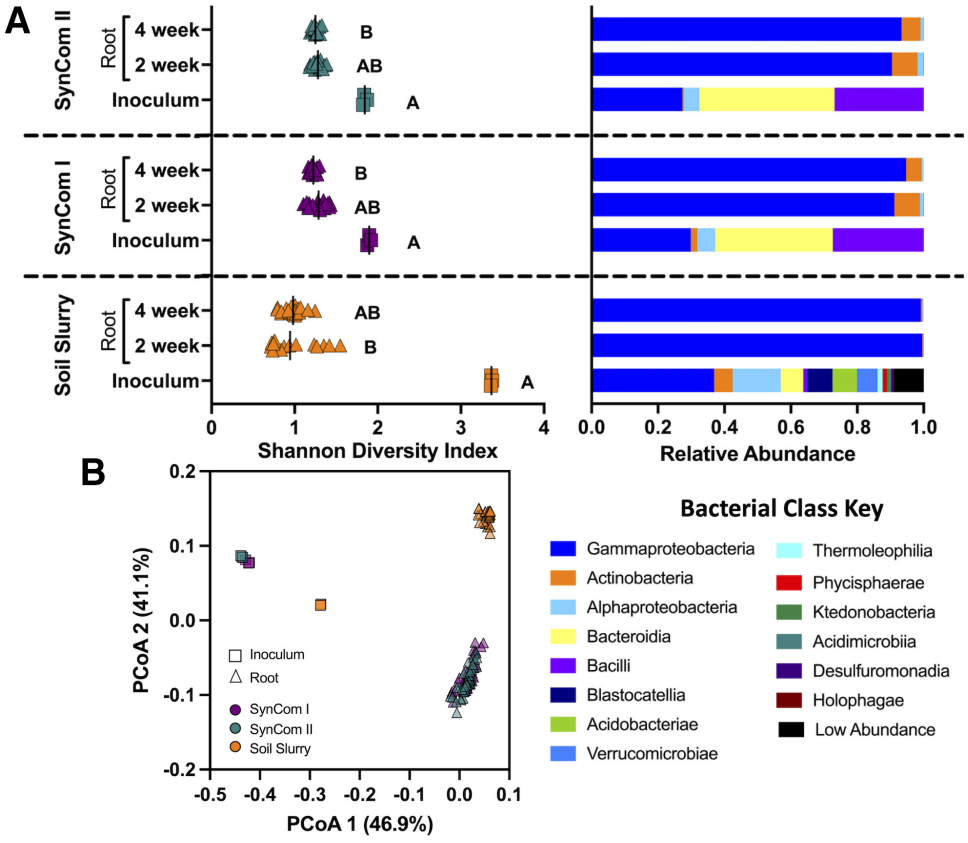

Fig. 1. *Arabidopsis* roots assemble subsets of microbes from both natural and constructed inocula. **A,** Shannon diversity calculations (left) and class level relative abundance (right) of taxa from root samples types and their corresponding inoculum. Within each inoculum type, diversity was compared using a Kruskal-Wallis test with Dunn's multiple comparisons. For inocula, $n = 3$. For root samples, $n = 19$ to 20. Letters indicate statistically different groups at $P \leq 0.0042$. **B,** Principal coordinate analysis (PCoA) of soil slurry and synthetic community (SynCom) inocula (squares) and corresponding root (triangle) samples at both 2-week and 4-week timepoints. SynCom I contains the four *Streptomyces* strains while SynCom II does not.

mately 10 3-mm glass beads in a SPEX SamplePrep 1600 MiniG at 1,500 rpm for 5 min for 2-week samples and 8 min for 4-week samples. Plant homogenate was serially diluted and plated on selective or differential solid media for CFU counts. All monoinoculated and *Streptomyces*-inoculated plant homogenates were plated on LB medium. Coinoculated plant homogenates were plated on media as follows: *Agrobacterium* sp. 33 on MacConkey and M9 minimal salts with 10% phenylalanine media, *Arthrobacter* sp. 131 on LB medium, *Burkholderia* sp. CL11 on LB and LB with nalidixic acid media at 15 μg/ ml, and *Ralstonia* sp. CL21 on M9 minimal salts with 10% myo-inositol and LB with streptomycin media at 50 μg/ ml. Although, *Arthrobacter* sp. 131 and the four *Streptomyces* strains were both plated on LB medium, their different colony morphologies allowed them to be distinguished from each other. CFU counts were normalized by plant biomass.

SA measurements. For in vivo SA levels in mono- and coinoculated plant tissue, experiments were repeated as described above with 10 seedlings for 2-week samples and 5 seedlings for 4-week samples combined to obtain the required 100 mg of tissue for each replicate. Combined seedling tissue was harvested, snap frozen, and stored at −80°C until the assay was performed. SA in whole plant tissue was measured according to the biosensor method described by DeFraia et al. (2008). Briefly, 100 mg of plant tissue was homogenized with approximately 5 3-mm glass beads in 500 μl of acetate buffer (0.1M, pH 5.6), which was sufficient liquid to fully homogenize plant tissue. Crude extract was separated from cell debris by centrifugation at 16,000 × *g*. Half of the crude extract

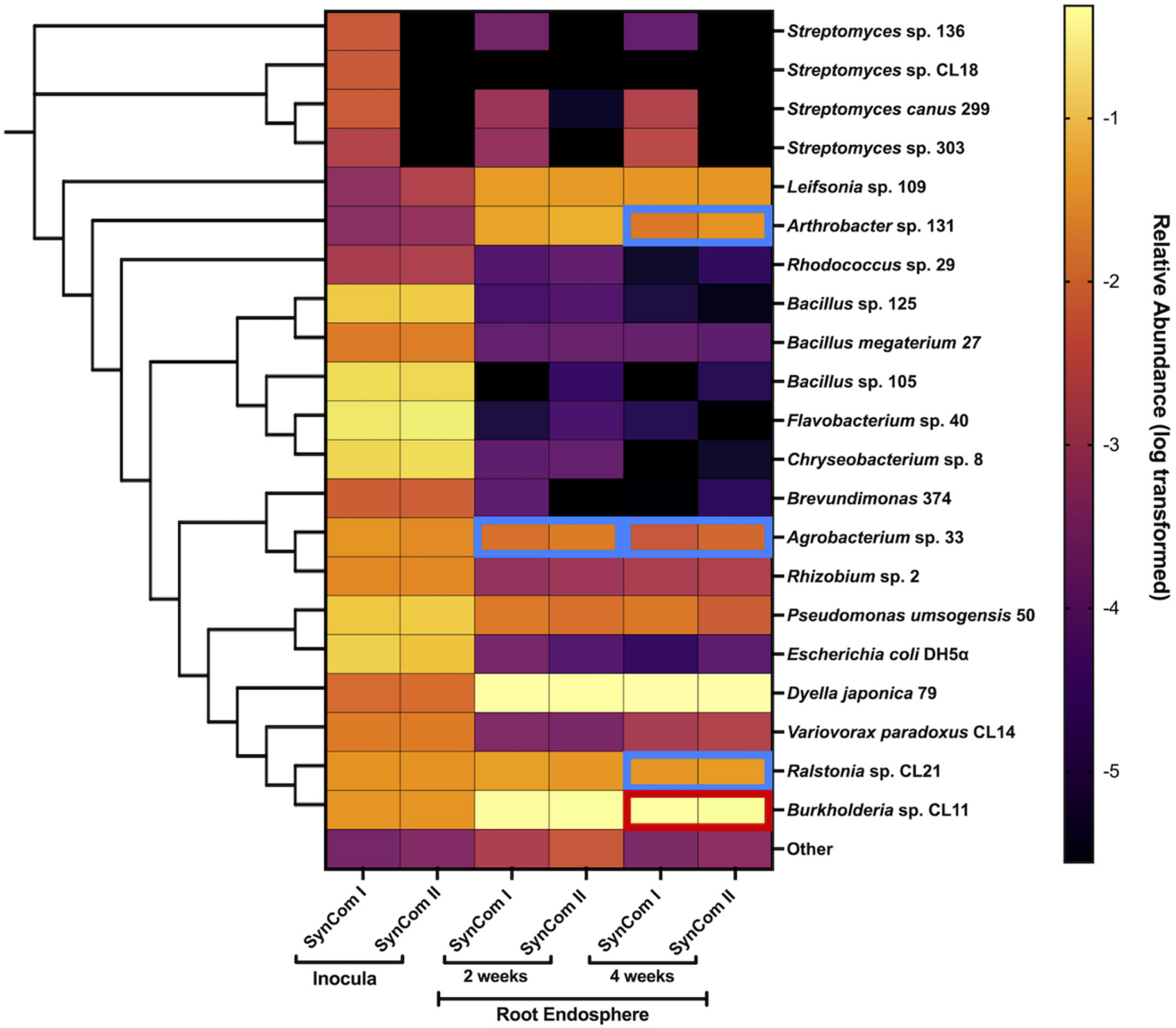

Fig. 2. Synthetic community (SynCom) members differ in their root microbiome abundance. Relative abundance (log-transformed values) for SynCom members calculated for inocula and root samples. CNVRG identified differentially abundant SynCom members, where *P* values > 0.95 predicted lower abundance and *P* values < 0.05 predicted higher abundance in SynCom I, which includes *Streptomyces* strains. Samples outlined in blue represent higher abundance in SynCom II compared with SynCom I: *Arthrobacter* sp. 131 ($P = 1$), *Agrobacterium* sp. 33 ($P = 0.971$ and $P = 0.984$), and *Ralstonia* sp. CL21 ($P = 0.954$). *Burkholderia* sp. CL11 outlined in red represents lower abundance in SynCom II compared with SynCom I ($P = 0.000684$). Phylogenetic tree was constructed from the *rpoB* gene sequences encoded by each SynCom member.

was treated with β-glucosidase to measure SA stored as SA 2-O-β-D-glucoside. Following β-glucosidase incubation, both treated and untreated crude extracts, along with standard concentrations of SA, were incubated with the luminescence biosensor *Acinetobacter* sp. ADPWH_*lux* and luminescence was read on a BioTek Synergy H1 Hybrid Multi-Mode micro plate reader. Although the standard curve of SA concentrations (0 to 1 µg) produced measurable luminescence, all plant samples were below the limit of detection.

SA growth curves. Isolates *Arthrobacter* sp. 131, *Agrobacterium* sp. 33, *Burkholderia* sp. CL11, and *Ralstonia* sp. CL21 were grown in LB at 30°C in a shaking incubator at 150 rpm for 2 days, until cultures were turbid. Cells were pelleted at 17,000 × *g* for 4 min, washed three times in sterile 1× PBS, and diluted to OD_{600} of 0.01 in one-fifth strength LB. SA dilutions were prepared in harvesting phosphate buffer to concentrations of 0.25, 0.5, and 1 mM. Normalized culture (100 µl) was put into a 96-well plate followed by 100 µl of SA dilutions or harvest phosphate buffer to create final SA concentrations of 0, 0.125, 0.25, and 0.5 mM, as previously performed by Lebeis et al. (2015). The 96-well plate was read in a BioTek Epoch 2 micro plate reader set to 30°C with continuous orbital shake that was run for 72 h, taking a reading every 2 h. Each isolate was grown in triplicate in each SA concentration. This experiment was repeated twice.

In vitro microbial interactions. In vitro microbial interaction assays were adapted from Vargas-Bautista et al. (2014). Isolates *Arthrobacter* sp. 131, *Agrobacterium* sp. 33, *Burkholderia* sp. CL11, *Ralstonia* sp. CL21, and the four *Streptomyces* strains and were grown for 2 to 7 days in LB at 30°C in a shaking incubator at 150 rpm, until cultures were turbid or displayed bacterial aggregates. *Streptomyces* cultures were pelleted at 17,000 × *g* for 4 min, washed three times in sterile 1× PBS, and diluted to OD_{600} of 0.1 in 1× PBS. Spots of the 0.1 OD_{600} *Streptomyces* mixture (15 µl each) were placed on 1/10th-strength solid LB media. Plates were grown overnight at 28°C because *Streptomyces* spp. grow at a slower rate than the other isolates. The following day, isolates *Arthrobacter* sp. 131, *Agrobacterium* sp. 33, *Burkholderia* sp. CL11, and *Ralstonia* sp. CL21 were pelleted at 17,000 × *g* for 4 min, washed three times in sterile 1× PBS, and diluted to OD_{600} of 0.1 in 1× PBS. Spots of the 0.1 OD_{600} cultures (15 µl each) were placed perpendicular to the *Streptomyces* spots. Plates were incubated at 28°C and growth was examined over 9 days.

Statistical analyses. Results for Figures 1, 2, 3, 4, and 5 were analyzed in Prism version 9.3.1 for macOS (GraphPad Software, La Jolla, CA, U.S.A.) (www.graphpad.com). Simpson's Diversity Index was compared within inoculation type (soil slurry, SynCom I, or SynCom II) using a Kruskal-Wallis test with Dunn's multiple comparison test. Coinoculation comparisons were performed using a Mann-Whitney test for CFU counts of one microbial isolate in monoinoculation versus coinoculation. Growth curves were analyzed at 36 h for an isolate in the four SA concentrations using a Kruskal-Wallis test with Dunn's multiple comparison test. Area under the curve (AUC) was calculated for each replicate and averaged to obtain a mean AUC with standard error. AUCs were compared using a Kruskal-Wallis test with Dunn's multiple comparison test.

RESULTS

***Arabidopsis* roots assemble subsets of microbes from both natural and constructed inocula into microbiomes.** To investigate *Streptomyces*-driven microbial interactions during endosphere assembly, we constructed two SynComs with (SynCom I) and without (SynCom II) *Streptomyces* strains that represent the dominant phyla found in root endospheres (Supplementary Table S1). To evaluate the impact of these communities on plant physiology, axenic *Arabidopsis* seedlings were inoculated with a slurry derived from natural soil (soil slurry) or one of the two constructed SynComs. After 2 or 4 weeks of growth, shoot and root biomass was assessed for inoculated plants as well as axenic control plants. At both timepoints, shoot and root biomass was significantly higher for plants inoculated with either SynCom compared with axenic controls (Supplementary Fig. S1). However, only 4-week root biomass was significantly higher than axenic plants for soil slurry-inoculated samples (Supplementary Fig. S1). To determine whether increased biomass influenced plant fitness, we evaluated seeds per silique as a proxy for plant fitness. However, no differences were detected between inoculated and axenic plants (Supplementary Fig. S2). Together, these results indicate both SynComs induce similar plant phenotypes as soil slurry samples, causing no fitness disadvantages. Furthermore, *Streptomyces* presence in SynCom I did not alter the plant outcomes when compared with SynCom II.

Because root endosphere communities consistently exhibit lower diversity than the surrounding soil, which is driven by enrichment and depletion of particular taxa, we hypothesized that assembled root endosphere microbiomes would be less diverse than soil slurry or SynCom inocula. As predicted, these internal root communities had reduced diversity when compared with their respective inocula (Fig. 1A, left). Furthermore, assembled root communities displayed similar abundances at the bacterial class level among all three inoculation types, with all root samples dominated by *Gammaproteobacteria* (Fig. 1A, right). When we generated weighted UniFrac

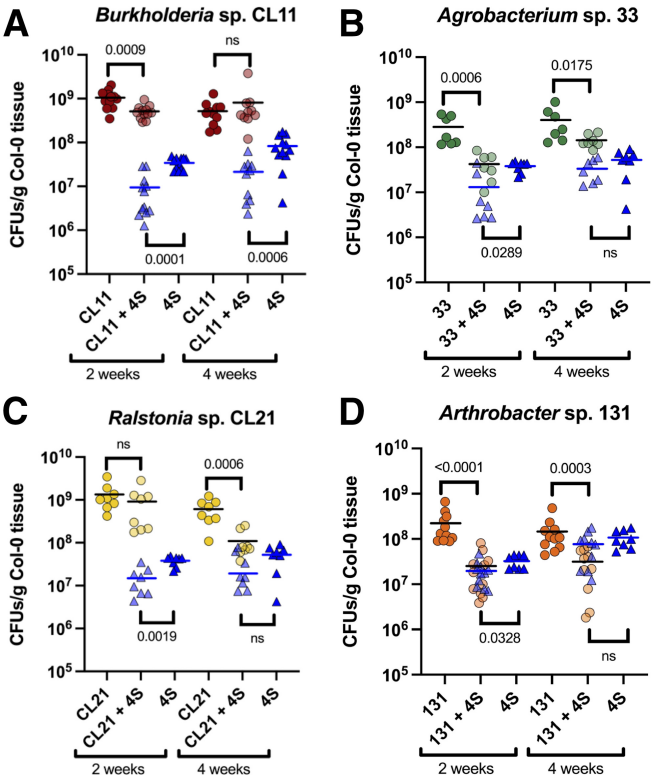

Fig. 3. Specific strains have lower whole-seedling colonization with *Streptomyces* coinoculation. **A,** *Burkholderia* sp. CL11; **B,** *Agrobacterium* sp. 33; **C,** *Ralstonia* sp. CL21; and **D,** *Arthrobacter* sp. 131. CFU counts were normalized by plant biomass for Col-0 seedlings inoculated with either single strains (indicated by strain number), the four *Streptomyces* strains (4S), or the combination of five strains (indicated by strain number followed by "+ 4S" ($n = 7$ to 12). Paired comparisons were calculated between monoinoculated CFUs and coinoculated CFUs for the same strains using a Mann-Whitney Test.

distances based on ASV abundance, we observed that root endosphere communities were distinguishable from each of their inoculum, and SynCom inocula samples were also distinct from soil slurry inocula samples (Fig. 1B). In this total community analysis, we failed to observe a separation between SynCom I and SynCom II samples (Fig. 1B). Interestingly, SynCom no-plant control samples were also dominated by *Gammaproteobacteria* and clustered closer to soil slurry root samples than inocula or SynCom root samples (Supplementary Fig. S3). Although we hypothesized that shifts would occur in endosphere community composition over time, no major differences were detected between 2 and 4 weeks postinoculation (Fig. 1). From our community analysis, we conclude that, although plants inoculated with soil slurry assemble root communities distinguishable from those inoculated with SynCom, the overall resulting structure in all root samples is similar in dynamics, with decreased diversity and dominance by *Gammaproteobacteria*.

Specific community members display altered endosphere abundance between SynCom I and SynCom II. To examine strain-specific differences between the two SynComs, we determined relative abundance for each community member in each root endosphere sample. Inoculation with either SynCom resulted in communities dominated by the same two *Gammaproteobacteria*, *Burkholderia* sp. CL11 and *Dyella japonica* 79 (Fig. 2). Interestingly, only *Burkholderia* sp. CL11 dominated the no-plant control samples (Supplementary Fig. S4), suggesting that *D. japonica* 79 abundance is positively influenced by *Arabidopsis* presence. To identify members consistently enriched in SynCom-inoculated root samples, we employed indicator species analysis (R package indicspecies) (Supplementary Table S1). This analysis also revealed particular SynCom members that were indicators of inocula samples, which we categorized as "poor" colonizers, because their abundance is lower in root samples than inocula (Supplementary Table S1). Indeed, these strains had no or low reads in noninoculum samples (Fig. 2; Supplementary Fig. S5A). These results revealed colonization differences among the less abundant SynCom members.

Although we hypothesized that the presence of *Streptomyces* in SynCom I would alter the abundance of specific community members in the endosphere when compared with SynCom II-inoculated roots, we failed to detect differences in community member abundances between SynCom I and SynCom II using indicator species analysis. We predicted that this was due to the low abundance and diversity of the root endosphere samples inoculated with SynCom. Therefore, we chose to employ Dirichlet-multinomial modeling analysis (R package CNVRG) (Harrison et al. 2020). From this modeling, four SynCom members were identified as differentially abundant between root samples inoculated with SynCom I compared with SynCom II: *Arthrobacter* sp. 131, *Agrobacterium* sp. 33, *Ralstonia* sp. CL21, and *Burkholderia* sp. CL11 (Fig. 2; Supplementary Table S2). This finding suggests that their abundance in the endosphere could be influenced by *Streptomyces*. The CNVRG differential abundance testing predicted that *Arthrobacter*

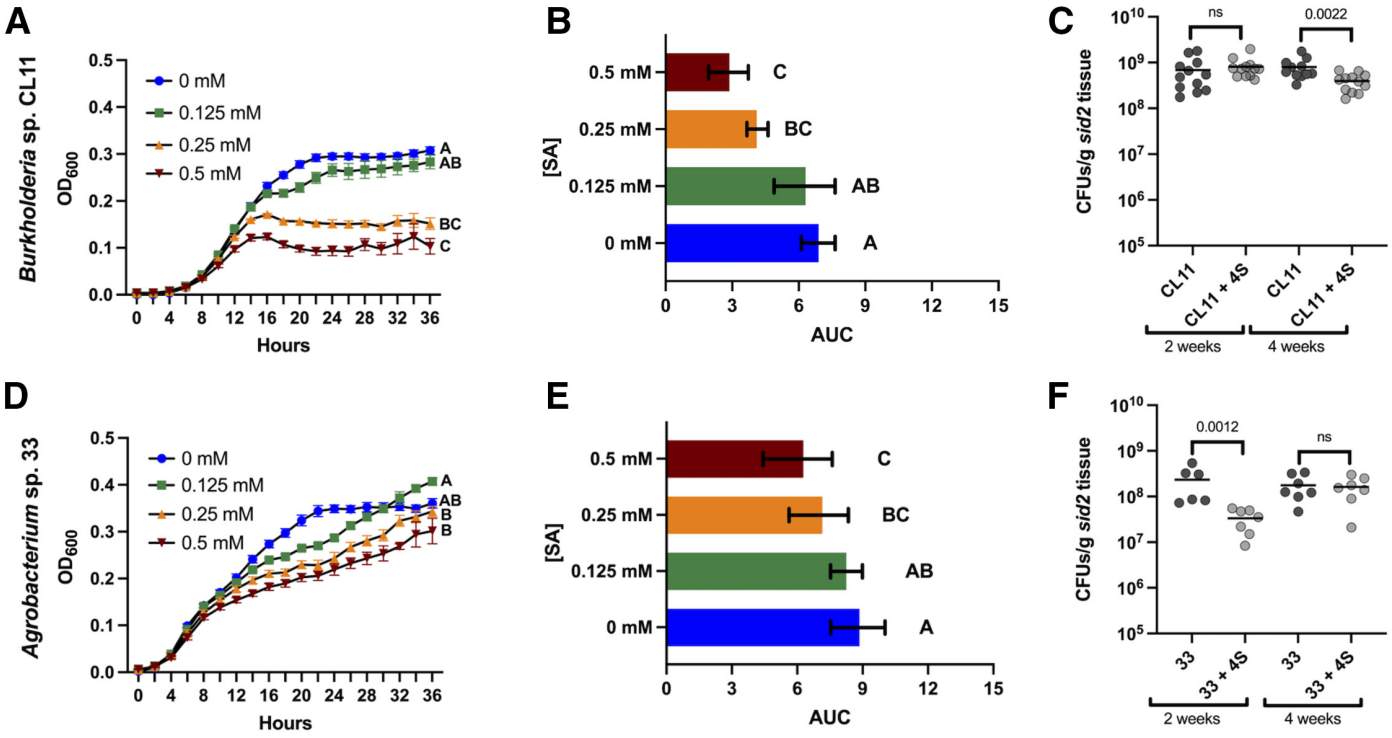

Fig. 4. Salicylic acid (SA) affects in vitro growth and seedling colonization for **A, B, and C,** *Burkholderia* sp. CL11 and **D, E, and F,** *Agrobacterium* sp. 33. **A and D,** Growth curves after 36 h in buffered 1/10th-strength Lysogeny broth media supplemented with 0 mM (blue circles), 0.125 mM (green squares), 0.25 mM (orange upward triangles), or 0.5 mM (red downward triangles) SA. Mean averages of three replicates for each data point are displayed with standard error bars. OD_{600} = optical density at 600 nm. Comparisons are shown for 36-h timepoint using a Kruskal-Wallis test with Dunn's multiple comparisons. Letters indicate statistically significant different at $P \leq 0.0256$ for *Burkholderia* sp. CL11 and $P \leq 0.0374$ for *Agrobacterium* sp. 33. **B and E,** Area under the curve (AUC) for associated growth curves for each isolate. Mean averages of each AUC are shown for three replicates with standard error bars. Comparisons were performed using a Kruskal-Wallis test with Dunn's multiple comparisons. Letters indicate statistically different groups at $P \leq 0.0478$ for *Burkholderia* sp. CL11 and $P \leq 0.0291$ for *Agrobacterium* sp. 33. **C and F,** CFU counts were normalized by seedling biomass from monoinoculated and coinoculated *sid2* plant tissue. Comparisons were calculated between monoinoculated CFUs and coinoculated CFUs for the same strains using a Mann-Whitney Test. For monoinoculation experiments, $n = 6$ to 12. For coinoculation experiments, $n = 7$ to 12.

sp. 131, *Agrobacterium* sp. 33, and *Ralstonia* sp. CL21 each had lower relative abundance in SynCom I-inoculated roots at 4 weeks, with *Agrobacterium* sp. 33 also predicted to have lower relative abundance in SynCom I-inoculated roots after 2 weeks (Fig. 2, blue boxes). Conversely, *Burkholderia* sp. CL11 was predicted to have higher relative abundance in SynCom I-inoculated roots after 4 weeks (Fig. 2, red box). Importantly, these four SynCom members were not defined as poor colonizers from indicator species analysis, supporting the idea that these microbial interactions could take place during root microbiome assembly. Because the differences in relative abundances were subtle (Fig. 2; Supplementary Fig. S5), we performed seedling coinoculation experiments with the four *Streptomyces* strains and the four differentially abundant members to directly test these predictions.

In vivo seedling coinoculations reflect in silico model predictions from root amplicon sequencing. To understand actual colonization outcomes from sequencing-based CNVRG predictions, we performed seedling coinoculation experiments and CFU analysis of the *Streptomyces* strains and predicted differentially abundant members. Although most differences were only predicted at 4 weeks postinoculation, plants were harvested at both 2 and 4 weeks postinoculation to expand our testing beyond confirming model predictions. These comparisons of monoinoculation and coinoculation colonization levels allowed us to focus on the direct influence of *Streptomyces* presence on *Burkholderia* sp. CL11, *Agrobacterium* sp. 33, *Ralstonia* sp. CL21, and *Arthrobacter* sp. 131 in the absence of other SynCom members.

Although it was predicted that the abundance of *Burkholderia* sp. CL11 would increase in the presence of *Streptomyces* at 4 weeks, we failed to detect a significant increase in CFUs (Fig. 3A). However, it was the only isolate tested that was not significantly lower in the coinoculation treatments compared with monoinoculation treatments at 4 weeks (Fig. 3). Among the three strains with predicted decreased abundance when *Streptomyces* spp. are present, two are *Proteobacteria* representatives (*Agrobacterium* sp. 33 and *Ralstonia* sp. CL21) and one is *Actinobacteria* (*Arthrobacter* sp. 131). As predicted from modeling, coinoculations of *Agrobacterium* sp. 33 and the *Streptomyces* strains resulted in significantly fewer *Agrobacterium* sp. 33 CFUs recovered from plant tissue at both timepoints when compared with *Agrobacterium* sp. 33 monoinoculated plants (Fig. 3B). In coinoculations of *Ralstonia* sp. CL21 and the *Streptomyces* strains, a significant decrease in *Ralstonia* CFUs was found when compared with monoinoculation at 4 weeks but not 2 weeks, which again confirmed the CNVRG differential abundance modeling predictions (Fig. 3C). In experiments with *Arthrobacter* sp. 131 and the *Streptomyces* strains, we found a significant reduction in *Arthrobacter* sp. 131 CFUs recovered from coinoculated plants as compared with monoinoculated plants at both 2 and 4 weeks postinoculation (Fig. 3D), although the model only predicted this difference after 4 weeks (Fig. 2).

Although most model predictions based on root relative abundances were supported by whole-seedling CFU counts, there were a handful of incongruent results highlighting the importance of in vivo examination of modeling results from amplicon sequencing

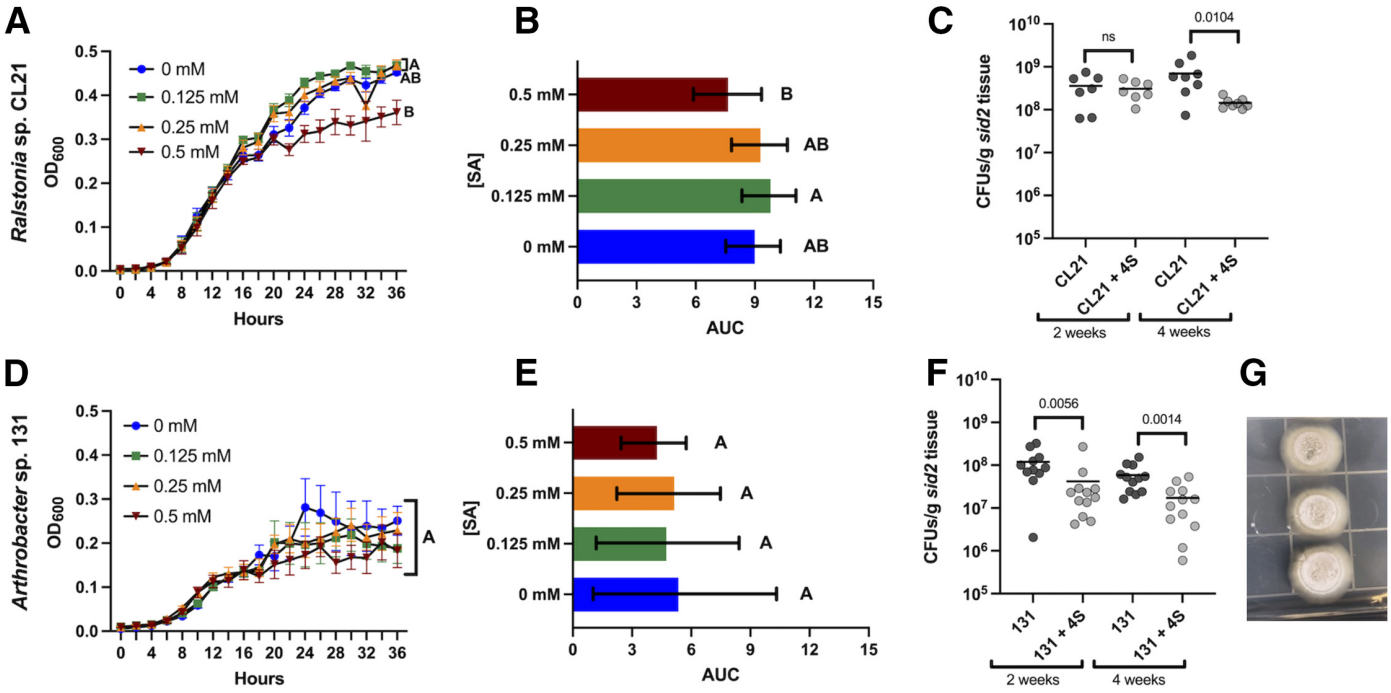

Fig. 5. Salicylic acid (SA) does not affect in vitro growth or seedling colonization for **A, B, and C,** *Ralstonia* sp. CL21 and **D, E, and F,** *Arthrobacter* sp. 131. **A and D,** Growth curves after 36 h in buffered 1/10th-strength Lysogeny broth (LB) media supplemented with 0 mM (blue circles), 0.125 mM (green squares), 0.25 mM (orange upward triangles), or 0.5 mM (red downward triangles) SA. Mean averages of three replicates of cultures for each data point are displayed with standard error bars. OD_{600} = optical density at 600 nm. Comparisons for the 36-h timepoint were made using a Kruskal-Wallis test with Dunn's multiple comparisons. Letters indicates significantly different at $P \leq 0.0087$ for *Ralstonia* sp. CL21. **B and E,** Area under the curve (AUC) for associated growth curves for each isolate. Averages of each AUC are shown for three replicates of cultures. Error bars represent the standard error of those AUCs. Comparisons performed using a Kruskal-Wallis test with Dunn's multiple comparisons. Letters indicate statistically different groups at $P \leq 0.0005$ for *Ralstonia* sp. CL21. **C and F,** CFU counts were normalized by seedling biomass from monoinoculated and coinoculated *sid2* plant tissue. Comparisons were calculated between monoinoculated CFUs and coinoculated CFUs for the same strains using a Mann-Whitney test. For colonization experiments, $n = 7$ to 12. **G,** Antibiosis of the four *Streptomyces* strains (center) on *Arthrobacter* sp. 131 (left and right) was observed on 1/10th-strength LB solid medium. Photos shown were taken after 9 days of growth.

data. This could be partially caused by the *Streptomyces* strain colonization levels in these sets of samples. In experiments where CNVRG predictions were not confirmed or interactions occurred that CNVRG did not predict, there were significantly fewer *Streptomyces* CFUs in coinoculated tissue compared with monoinoculated tissue (Fig. 3). Previously mentioned mechanisms such as niche competition could account for differences in *Streptomyces* colonization in monoinoculated compared with coinoculated tissue. However, this would require further investigation. Because the four *Streptomyces* strains individually differed in their ability to colonize seedlings, partially due to exogenous SA application, we chose to explore the immune system influence on these tested microbial interactions (Chewning et al. 2019; Lebeis et al. 2015).

Differential impacts of host-produced SA on microbial interactions and colonization outcomes. Previously, SA was determined to mediate root endosphere community assembly (Lebeis et al. 2015). The four *Streptomyces* strains in this SynCom were found to be differentially sensitive to SA addition to in vitro growth (Chewning et al. 2019). Moreover, among the four *Streptomyces* strains, one was enriched in the *Arabidopsis* mutant lacking the first enzyme in SA production, *sid2*, while another was found to be enriched in exogenously treated SA-treated plants (Lebeis et al. 2015). To understand how the plant immune system might modulate microbial interactions and subsequent colonization, we investigated how SA affects the in vitro growth and seedling colonization for our SynCom members of interest.

To examine whether SA altered the in vitro growth of the differentially abundant SynCom members, we performed in vitro growth assays in buffered media with SA concentrations ranging from 0 to 0.5 mM SA. Both *Burkholderia* sp. CL11 and *Agrobacterium* sp. 33 showed negatively altered growth in the presence of SA (Fig. 4). *Burkholderia* sp. CL11 displayed SA sensitivity in vitro because the maximum OD of cultures with 0.25 or 0.5 mM SA was significantly lower than cultures with 0 mM SA (Fig. 4A). *Agrobacterium* sp. 33 displayed delayed growth with increasing concentrations of SA, with the 0- and 0.125-mM cultures reaching a higher OD than cultures with 0.25 or 0.5 mM SA (Fig. 4D). To further understand the different impacts of SA on *Burkholderia* sp. CL11 and *Agrobacterium* sp. 33 in vitro growth, we calculated growth rates for these strains during early to mid-exponential phase (4 to 12 h). We selected these times points because they included exponential growth for both isolates in all four concentrations of SA. For *Burkholderia* sp. CL11, growth rates (k) of cultures decreased with increasing SA, while doubling time increased (Supplementary Table S3). Although *Agrobacterium* sp. 33 also displayed decreased growth rates and increased doubling time with increasing SA, results were more subtle than changes to *Burkholderia* sp. CL11 growth (Supplementary Table S3). Taken together, these results demonstrate that *Burkholderia* sp. CL11 and *Agrobacterium* sp. 33 exhibited direct negative SA-influenced phenotypes on in vitro growth (Fig. 4).

To determine whether this in vitro SA influence was relevant to the SA concentrations that microbes experience during seedling colonization, we attempted in planta SA quantification from monoinoculated and coinoculated plant tissue (DeFraia et al. 2008). However, levels of SA within these inoculated plant tissues were below the limit of detection at 2 and 4 weeks postinoculation (data not shown), although it remained possible that plant SA biosynthesis contributes to colonization phenotypes at earlier timepoints. Therefore, we conducted monoinoculation and coinoculation experiments in *sid2* plants. Interestingly, *Burkholderia* sp. CL11-inoculated *sid2* plants showed delayed colonization phenotypes compared with inoculated Col-0 plants (Fig. 4C). In Col-0, *Burkholderia* sp. CL11 colonization was higher in monoinoculated than coinoculated plant tissue at 2 weeks but not 4 weeks whereas, in *Arabidopsis sid2*, its colonization was higher in monoinoculated than coinoculated plant tissue only at 4 weeks (Fig. 4C). In Col-0, *Agrobacterium* sp. 33 displayed significantly reduced CFUs from coinoculated tissue compared with monoinoculated tissue at both harvest timepoints (Fig. 3). Although this phenotype was consistent in *sid2* plants at 2 weeks, it did not extend to 4 weeks postinoculation, suggesting that host SA alters later colonization (Fig. 4B). These results demonstrate that SA affected both in vitro microbial growth and long-term plant colonization outcomes. However, these SynCom members responded to in vitro and in vivo SA differently.

When we investigated SA influence on the in vitro growth of *Arthrobacter* sp. 131 and *Ralstonia* sp. CL21, we found that their overall growth was not affected by addition of SA to the media (Fig. 5). Furthermore, neither strain displayed colonization phenotypes influenced by host SA production (Fig. 5). The significantly lower CFU recovery when *Streptomyces* spp. were present after 4 weeks (Fig. 3) was consistent between Col-0 and *sid2* for both *Arthrobacter* sp. 131 and *Ralstonia* sp. CL21 (Fig. 5). Together, these in vitro and in vivo data suggest that SA does not mediate the decreased colonization of these two SynCom members. However, we observed inhibition of *Arthrobacter* sp. 131 growth by the four *Streptomyces* strains in vitro, suggesting that direct antibiosis by these *Streptomyces* strains could account for lower colonization levels (Fig. 5G). Among the differentially abundant strains, this strong growth inhibition was unique to *Arthrobacter* sp. 131 because each of the other three strains was able to form overlapping colonies with the *Streptomyces* strains (Supplementary Fig. S7). It is worth noting that colonization differences in monoinoculations in Col-0 compared with *sid2* plants were found at varying timepoints for all members except *Agrobacterium* sp. 33 (Supplementary Fig. S6). Exploration of whether this is due to direct bacteriostatic activity of SA or the downstream effects it triggers will be needed to resolve the influence of SA on microbiome assembly and microbial interactions. Overall, our results showed varying colonization phenotypes identified from amplicon sequencing data that are mediated by different mechanisms directed by the plant host and microbial effects.

DISCUSSION

Due to the complex nature of plant microbiome assembly, it is difficult to dissect host- and microbial-derived mechanisms from one another to understand how each affects community composition. SynComs are an experimental approach that facilitate mechanistic understanding of microbial interactions during plant microbiome assembly (Carlström et al. 2019; Niu et al. 2017). Here, we utilized two SynComs to elucidate the effects of *Streptomyces* strains on endosphere community composition because this genus has been shown to influence the growth of other microbes (Cordovez et al. 2015). Our plant physiology and microbiome characterizations showed that both SynComs induced similar host outcomes (Supplementary Figs. S1 and S2) and overall endosphere microbiome structure (Fig. 1), which was likely driven by the dominant members in root samples *Burkholderia* sp. CL11 and *D. japonica* 79. However, four specific SynCom members were predicted to differ in abundance between the two SynComs (Fig. 2). Relative abundance calculated from amplicon sequencing data relies on SynCom size, abundance of other organisms, and 16S rRNA gene copy number of SynCom members (Gloor et al. 2017; Kembel et al. 2012; Vorholt et al. 2017). Although shifts in community composition could be due to the smaller community size of SynCom II, we hypothesized that this would not be the case for all CNVRG predictions, because *Burkholderia* sp. CL11 was predicted to have higher

relative abundance in SynCom I, which is the larger community (Fig. 2). Therefore, we employed seedling coinoculation experiments with the four *Streptomyces* strains and differentially abundant members to test altered abundances with actual abundance quantification (CFUs).

Although most of the coinoculation colonization results support the accuracy of the interactions identified in SynCom experiments by CNVRG, we failed to detect a significant increase in the CFUs recovered from 4-week *Burkholderia* sp. CL11 coinoculated plant tissue (Fig. 3). Furthermore, we observed significantly fewer *Burkholderia* sp. CL11 and *Arthrobacter* sp. 131 CFUs from coinoculated tissue than monoinoculated tissue at 2 weeks (Fig. 3), which was not predicted from our amplicon sequencing data. These results emphasize the need to experimentally test hypotheses generated from amplicon sequencing. Furthermore, this highlights the idea that we cannot ignore the effects of other microbial interactions within the SynCom. Although other SynCom members do not colonize the endosphere at high levels (Figs. 1 and 2; Supplementary Fig. S5), the results shown with *Streptomyces* strains in this work demonstrate that their influence on other microbes does not correlate to their abundance in the community (Figs. 2 and 3). Together, these interactions that differed from CNVRG predictions show the importance of examining predicted community interactions during microbiome assembly.

Previously, SA was found to mediate root microbiome assembly in soil and SynCom-inoculated plants (Lebeis et al. 2015). Specific SynCom members were found to have differential abundance in SA-altered *Arabidopsis* genotypes and SA-treated plants that corresponded to their in vitro growth response to SA (Lebeis et al. 2015). This demonstrated a direct role of SA during microbiome assembly. Furthermore, SA has been implicated in the differential *Arabidopsis* colonization of the four *Streptomyces* strains used in this study (Chewning et al. 2019). Although it remains unclear how SA mechanistically contributes to microbial interactions during root microbiome assembly, here, we identified cases in which SA affects microbial interactions as well as instances which it did not. In these studies, we found that *Burkholderia* sp. CL11 and *Agrobacterium* sp. 33 were sensitive to SA during in vitro growth (Fig. 4). While seedling coinoculation experiments performed in *Arabidopsis sid2* revealed that SA influenced colonization phenotypes for these two members (Fig. 4), host SA production affected these two strains differently. In vitro, *Burkholderia* sp. CL11 was significantly affected by the two highest SA concentrations, while *Agrobacterium* sp. 33 showed delayed growth. Although we saw direct SA influence in growth curve experiments, in vivo colonization demonstrated an indirect SA-influenced phenotype (Fig. 4). While coinoculation experiments in *Arabidopsis sid2* for these SynCom members were different from results in *Arabidopsis* Col-0, monoinoculations for *Burkholderia* sp. CL11 and *Agrobacterium* sp. 33 did not vary greatly between the two genotypes (Supplementary Fig. S6). We hypothesize that these interactions are both *Streptomyces* dependent and plant dependent, likely influenced by downstream SA signaling.

In contrast, *Ralstonia* sp. CL21 and *Arthrobacter* sp. 131 were found to be largely resistant to in vitro growth with SA addition to the liquid media. Additionally, *sid2* seedling colonization was not different from Col-0 colonization, suggesting that they are not influenced by host SA production. These results highlight the differential influence of SA on microbiome members. In vitro microbial interaction assays revealed inhibition of *Arthrobacter* sp. 131 growth by the four *Streptomyces* strains, indicating a potential mechanism for the reduction of *Arthrobacter* sp. 131 CFUs in coinoculation experiments (Fig. 5G). We hypothesize that small colonies of *Arthrobacter* sp. 131 that grew in the presence of the *Streptomyces* strains are satellite colonies, presumably mutant colonies that survived antibiotic pressure while the original strain was sensitive to the *Streptomyces* antibiosis (Medaney et al. 2016). However, further investigation of this is required. No inhibition of *Ralstonia* sp. CL21 by the four *Streptomyces* strains was seen (Supplementary Fig. S7). We hypothesize that the reduction of *Ralstonia* sp. CL21 recovered from coinoculated plants could be due to other mechanisms of microbial competition such as niche competition (Hassani et al. 2018).

Because SA levels in seedling tissues generated by this experimental setup were below our limit of detection (data not shown), we hypothesize that there is not sustained stimulation of the immune system by these nonpathogenic SynCom members. The influence of SA in seedling colonization could be amplification of early colonization SA induction, which is detectable within 24 h postinoculation with pathogens (Wildermuth et al. 2001). These results could also result from crosstalk of other plant defense mechanisms, which may be working in conjunction with or counteract SA to alter microbial interactions and subsequent colonization or the downstream responses that SA accumulation triggers (Shigenaga et al. 2017). Although SAR is an SA-dependent mechanism by which pathogens influence later microbial colonization, the SA-influenced microbial interactions we identified here were triggered by nonpathogens via unknown mechanisms. Overall, further exploration is needed to fully capture the complexity of host SA production on microbial interactions in the context of microbiome assembly.

Interestingly, these results demonstrate how *Streptomyces* spp. influence the colonization of 4 members within our 21-member SynCom. Moreover, these four interactions represented both SA-influenced and non-SA-influenced interactions. Due to their plant-growth-promotion characteristics and ability to influence other microbes, *Streptomyces* spp. are potential targets for microbial treatments for plants (Olanrewaju and Babalola 2019; Vurukonda et al. 2018). Although *Streptomyces* spp. have been frequently implemented in biocontrol and growth inhibition of other microbes (Olanrewaju and Babalola 2019; Vurukonda et al. 2018), *Streptomyces* antibiosis was only found for one member, *Arthrobacter* sp. 131, in our SynComs (Supplementary Fig. S7). This suggests that multiple mechanisms modulate *Streptomyces*-driven microbial interactions in the context of plant microbiome assembly. Our results indicate that use of *Streptomyces* spp. in agricultural settings may contribute to microbial interactions and alter the native soil microbiome via multiple mechanisms. Furthermore, consideration for how these mechanisms contribute to root resilience during and following biotic and abiotic stresses that trigger SA production in mature plants must also be explored in future studies.

In conclusion, inclusion of four *Streptomyces* strains in SynCom I altered the root abundance of specific members in larger community experiments. To understand the full scale of these results, predictions from amplicon sequencing data were examined using in vivo seedling coinoculation experiments. Overall, our coinoculation experiments validate the directionality of in vivo microbial interactions predicted from the amplicon sequencing dataset. Furthermore, our results suggest that these interactions are robust across abiotic conditions because the SynCom and coinoculation assays used distinct experimental systems. Among the microbial interactions predicted from amplicon sequencing and supported by seedling coinoculation experiments, our results distinguish direct *Streptomyces* antibiosis (e.g., *Arthrobacter* sp. 131) from indirect influence that requires host SA production to observe colonization differences (*Burkholderia* sp. CL11 and *Agrobacterium* sp. 33). The mechanisms and extent of SA influence in these microbial interactions during root microbiome assembly requires future investigation. Further research is needed to fully understand

how plant–microbe and microbe–microbe interactions work in concert during microbiome assembly for these interactions to be harnessed for successful plant microbiome treatments for use in agriculture.

Data availability. Raw sequences were deposited in the Sequence Read Archive under Bioproject accession number PRJNA895095.

ACKNOWLEDGMENTS

All SynCom isolates were originally isolated in the laboratory of Jeffery Dangl at the University of North Carolina. We thank Bridget S. O'Banion for advice on coinoculation experiments and contributions to text and Asia Hawkins for help with preparing experimental supplies.

LITERATURE CITED

Adamczak, A., Ożarowski, M., and Karpiński, T. M. 2020. Antibacterial activity of some flavonoids and organic acids widely distributed in plants. J. Clin. Med. 9:109.

Bodenhausen, N., Bortfeld-Miller, M., Ackermann, M., and Vorholt, J. A. 2014. A synthetic community approach reveals plant genotypes affecting the phyllosphere microbiota. PLoS Genet. 10:e1004283.

Boza, G., Worsley, S. F., Yu, D. W., and Scheuring, I. 2019. Efficient assembly and long-term stability of defensive microbiomes via private resources and community bistability. PLoS Comput. Biol. 15:e1007109.

Bulgarelli, D., Rott, M., Schlaeppi, K., Ver Loren van Themaat, E., Ahmadinejad, N., Assenza, F., Rauf, P., Huettel, B., Reinhardt, R., Schmelzer, E., Peplies, J., Gloeckner, F. O., Amann, R., Eickhorst, T., and Schulze-Lefert, P. 2012. Revealing structure and assembly cues for *Arabidopsis* root-inhabiting bacterial microbiota. Nature 488:91-95.

Carlström, C. I., Field, C. M., Bortfeld-Miller, M., Müller, B., Sunagawa, S., and Vorholt, J. A. 2019. Synthetic microbiota reveal priority effects and keystone strains in the *Arabidopsis* phyllosphere. Nat. Ecol. Evol. 3:1445-1454.

Chewning, S. S., Grant, D. L., O'Banion, B. S., Gates, A. D., Kennedy, B. J., Campagna, S. R., and Lebeis, S. L. 2019. Root-associated *Streptomyces* isolates harboring *melC* genes demonstrate enhanced plant colonization. Phytobiomes J. 3:165-176.

Compant, S., Samad, A., Faist, H., and Sessitsch, A. 2019. A review on the plant microbiome: Ecology, functions, and emerging trends in microbial application. J. Adv. Res. 19:29-37.

Cordovez, V., Carrion, V. J., Etalo, D. W., Mumm, R., Zhu, H., van Wezel, G. P., and Raaijmakers, J. M. 2015. Diversity and functions of volatile organic compounds produced by *Streptomyces* from a disease-suppressive soil. Front. Microbiol. 6:1081.

DeFraia, C. T., Schmelz, E. A., and Mou, Z. 2008. A rapid biosensor-based method for quantification of free and glucose-conjugates salicylic acid. Plant Methods 4:28.

Eckshtain-Levi, N., Harris, S. L., Roscios, R. Q., and Shank, E. A. 2020. Bacterial community members increase *Bacillus subtilis* maintenance on the roots of *Arabidopsis thaliana*. Phytobiomes J. 4:303-313.

Fitzpatrick, C. R., Copeland, J., Wang, P. W., Guttman, D. S., Kotanen, P. M., and Johnson, M. T. J. 2018. Assembly and ecological function of the root microbiome across angiosperm plant species. Proc. Natl. Acad. Sci. U.S.A. 115:E1157-E1165.

Gloor, G. B., Macklaim, J. M., Pawlowsky-Glahn, V., and Egozcue, J. J. 2017. Microbiome datasets are compositional: And this is not optional. Front. Microbiol. 8:2224.

Hacquard, S., Garrido-Oter, R., González, A., Spaepen, S., Ackermann, G., Lebeis, S., McHardy, A. C., Dangl, J. L., Knight, R., Ley, R., and Schulze-Lefert, P. 2015. Microbiota and host nutrition across plant and animal kingdoms. Cell Host Microbe 17:603-616.

Harrison, J. G., Calder, W. J., Shastry, V., and Buerkle, C. A. 2020. Dirichlet-multinomial modelling outperforms alternatives for analysis of microbiome and other ecological count data. Mol. Ecol. Resour. 20:481-497.

Hassani, M. A., Durán, P., and Hacquard, S. 2018. Microbial interactions within the plant holobiont. Microbiome 6:58.

Kembel, S. W., Wu, M., Eisen, J. A., and Green, J. L. 2012. Incorporating 16S gene copy number information improves estimates of microbial diversity and abundance. PLoS Comput. Biol. 8:e1002743.

Klindworth, A., Pruesse, E., Schweer, T., Peplies, J., Quast, C., Horn, M., and Glöckner, F. O. 2013. Evaluation of general 16S ribosomal RNA gene PCR primers for classical and next-generation sequencing-based diversity studies. Nucleic Acids Res. 41:e1.

Koo, Y. M., Heo, A. Y., and Choi, H. W. 2020. Salicylic acid as a safe plant protector and growth regulator. Plant Pathol J. 36:1-10.

Lebeis, S. L., Paredes, S. H., Lundberg, D. S., Breakfield, N., Gehring, J., McDonald, M., Malfatti, S., Glavina del Rio, T., Jones, C. D., Tringe, S. G., and Dangl, J. L. 2015. Salicylic acid modulates colonization of the root microbiome by specific bacterial taxa. Science 349:860-864.

Lundberg, D. S., Lebeis, S. L., Paredes, S. H., Yourstone, S., Gehring, J., Malfatti, S., Tremblay, J., Engelbrektson, A., Kunin, V., Glavina del Rio, T., Edgar, R. C., Eickhorst, T., Ley, R. E., Hugenholtz, P., Tringe, S. G., and Dangl, J. L. 2012. Defining the core *Arabidopsis thaliana* root microbiome. Nature 488:86-90.

Lundberg, D. S., Yourstone, S., Mieczkowski, P., Jones, C. D., and Dangl, J. L. 2013. Practical innovations for high-throughput amplicon sequencing. Nat. Methods 10:999-1002.

Medaney, F., Dimitriu, T., Ellis, R. J., and Raymond, B. 2016. Live to cheat another day: Bacterial dormancy facilitates the social exploitation of β-lactamases. ISME J. 10:778-787.

Niu, B., Paulson, J. N., Zheng, X., and Kolter, R. 2017. Simplified and representative bacterial community of maize roots. Proc. Natl. Acad. Sci. U.S.A. 114:E2450-E2459.

Olanrewaju, O. S., and Babalola, O. O. 2019. *Streptomyces*: Implications and interactions in plant growth promotion. Appl. Microbiol. Biotechnol. 103:1179-1188.

Pfeilmeier, S., Petti, G. C., Bortfeld-Miller, M., Daniel, B., Field, C. M., Sunagawa, S., and Vorholt, J. A. 2021. The plant NADPH oxidase RBOHD is required for microbiota homeostasis in leaves. Nat. Microbiol. 6: 852-864.

Shigenaga, A. M., Berens, M. L., Tsuda, K., and Argueso, C. T. 2017. Towards engineering of hormonal crosstalk in plant immunity. Curr. Opin. Plant Biol. 38:164-172.

Stringlis, I. A., Yu, K., Feussner, K., de Jonge, R., Van Bentum, S., Van Verk, M. C., Berendsen, R. L., Bakker, P. A. H. M., Feussner, I., and Pieterse, C. M. J. 2018. MYB72-dependent coumarin exudation shapes root microbiome assembly to promote plant health. Proc. Natl. Acad. Sci. U.S.A. 115:E5213-E5222.

Trivedi, P., Leach, J. E., Tringe, S. G., Sa, T., and Singh, B. K. 2020. Plant-microbiome interactions: From community assembly to plant health. Nat. Rev. Microbiol 18:607-621.

Vargas-Bautista, C., Rahlwes, K., and Straight, P. 2014. Bacterial competition reveals differential regulation of the *pks* genes by *Bacillus subtilis*. J. Bacteriol. 196:717-728.

Vatsa-Portugal, P., Aziz, A., Rondeau, M., Villaume, S., Morjani, H., Clément, C., and Ait Barka, E. 2017. How *Streptomyces anulatus* primes grapevine defenses to cope with gray mold: A study of the early responses of cell suspensions. Front Plant Sci. 8:1043.

Vlot, A. C., Sales, J. H., Lenk, M., Bauer, K., Brambilla, A., Sommer, A., Chen, Y., Wenig, M., and Nayem, S. 2021. Systemic propagation of immunity in plants. New Phytol. 229:1234-1250.

Voges, M. J. E. E. E., Bai, Y., Schulze-Lefert, P., and Sattely, E. S. 2019. Plant-derived coumarins shape the composition of an *Arabidopsis* synthetic root microbiome. Proc. Natl. Acad. Sci. U.S.A. 116:12558-12565.

Vorholt, J. A., Vogel, C. Carlström, C. I., and Müller, D. B. 2017. Establishing causality: Opportunities of synthetic communities for plant microbiome research. Cell Host Microbe 22:142-155.

Vurukonda, S. S. K. P., Giovanardi, D., and Stefani, E. 2018. Plant growth promoting and biocontrol activity of *Streptomyces* spp. as endophytes. Int. J. Mol. Sci. 19:952.

Wildermuth, M. C., Dewdney, J., Wu, G., and Ausubel, F. M. 2001. Isochorismate synthase is required to synthetize salicylic acid for plant defense. Nature 414:562-565.

Worsley, S. F., Macey, M. C., Prudence, S. M. M., Wilkinson, B., Murrell, J. C., and Hutchings, M. I. 2021. Investigating the role of root exudates in recruiting *Streptomyces* bacteria to the *Arabidopsis thaliana* microbiome. Front. Mol. Biosci. 8:686110.